ChemComm

COMMUNICATION

View Article Online
View Journal

Cite this: DOI: 10.1039/d5cc03180j

Received 5th June 2025,
Accepted 11th August 2025

DOI: 10.1039/d5cc03180j

rsc.li/chemcomm

A J-aggregating cyanine-based NIR-II optical sensor for DNA aptamer-mediated detection and imaging of quinine

Gaowei Deng, † Chaobang Zhang,† Jiawei Chen, Fang Zeng * and Shuizhu Wu *

We report a dye-displacement assay for quinine detection integrating a DNA aptamer with a J-aggregating NIR-II cyanine dye. This platform achieves sensitive, selective, and label-free NIR-II colorimetric and fluorescence sensing, with a fluorescence-based detection limit as low as 0.014 μM in urine solution, and enables NIR-II fluorescence imaging.

Aptamer-based sensors have emerged as powerful tools in analytical chemistry due to their high specificity, tuneable affinity, and compatibility with a wide range of targets, from small molecules to proteins and even whole cells.[1–3] By integrating DNA aptamers with optical reporters, a variety of signal transduction strategies can be realized, among which dye displacement assays have gained considerable attention.[4,5] In these systems, a reporter dye—often a small chromophore or fluorophore—is non-covalently associated with the aptamer through electrostatic or hydrophobic interactions. Upon target binding, the dye is competitively displaced due to the stronger affinity between the aptamer and its analyte, leading to changes in the dye's optical properties, such as absorption or fluorescence. These spectral changes can be directly correlated with analyte concentration, enabling rapid, label-free, and highly sensitive detection.[1c,6,7] Some aptamer–dye displacement systems have been developed for clinically and environmentally relevant targets. Recently, Xiao and coworkers developed a series of colorimetric assays based on aptamer–cyanine systems. Their approach allows for the detection of various small molecules, providing a rapid and sensitive method suitable for sensing applications.[7b–d]

While these platforms are elegant and adaptable, there is still room for improvement. For instance, the previously reported sensors operate in the visible and near-infrared I (NIR-I) range, which is suboptimal for biological applications due to high background autofluorescence and limited tissue penetration. In contrast, optical detection and imaging in the NIR-II range can substantially reduce the autofluorescence and improve tissue penetration. Moreover, many of the dye-aptamer systems are used as the colorimetric sensors, which generally exhibit relatively lower detection sensitivity compared to fluorescence detection.[8] Cyanine dyes, particularly those capable of forming supramolecular aggregates, are well suited for dye displacement assays due to their sharp spectral signatures and responsive optical behaviour.[7] Cyanine J-aggregates demonstrate distinct bathochromic shifts, enhanced molar absorptivity, and narrowed spectral linewidths compared to their monomeric counterparts, making them attractive for signal amplification in biosensing applications.[9] However, designing a cyanine dye capable of forming NIR-II J-aggregates is not an easy task, let alone obtaining stable J-aggregates that can function in biological media. Recently, we developed a strategy for constructing a series of cyanine-based J-aggregates with their absorption/emission spectra in the NIR-II region.[10]

Quinine remains a critical therapeutic agent for treating severe malaria. However, its narrow therapeutic window, potential toxicity, and inter-individual pharmacokinetic variability require precise monitoring in clinical and pharmacological settings.[11] Thus, sensitive and selective detection of quinine in biological fluids is essential.

In this study, we aimed to make use of our strategy to develop a displacement assay system capable of detecting quinine through target-triggered J-aggregate formation and associated spectral transitions. By screening our existing J-aggregating cyanines and designing new NIR-II cyanine J-aggregates, we successfully achieved NIR-II colorimetric and fluorescent detection and imaging of quinine in biological fluids. Our experiments also indicate that the limit of detection (LOD) of fluorescence assays is an order of magnitude lower

State Key Laboratory of Luminescent Materials and Devices, Guangdong Provincial Key Laboratory of Luminescence from Molecular Aggregates, School of Materials Science and Engineering, South China University of Technology, Guangzhou 510640, China. E-mail: mcfzeng@scut.edu.cn, shzhwu@scut.edu.cn
† These authors contributed equally in this study.

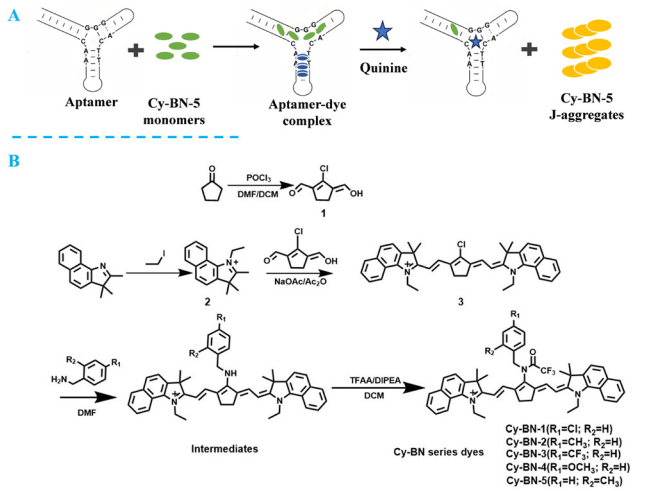

Scheme 1 (A) Schematic illustration of the assay of quinine using an aptamer-dye complex. (B) Synthetic route for cyanine dyes (Cy-BN-1 to Cy-BN-5).

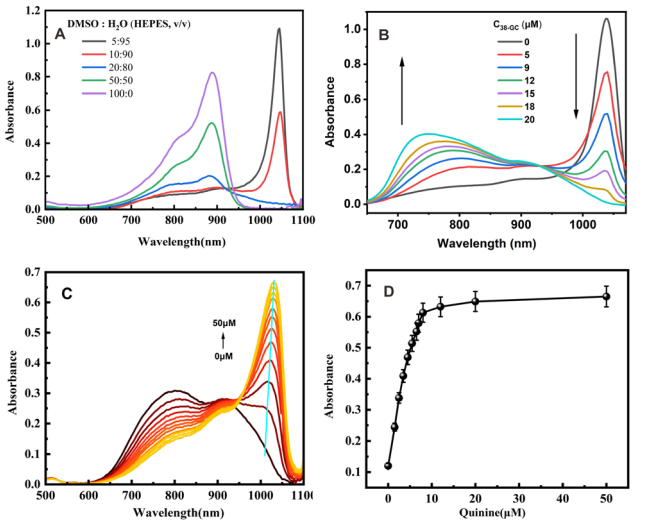

Fig. 1 (A) Absorption spectra of dye Cy-BN-5 in pH 7.4 HEPES solutions with varied ratios of DMSO to water. (B) Absorption spectra for Cy-BN-5 upon addition of aptamer 38-GC of varied concentrations. (C) Absorption spectra of Cy-BN-5/38-GC in pH 7.4 HEPES solution after addition into quinine solutions with varied concentrations (0, 1.5, 2.5, 3.5, 4.5, 5.5, 6.5, 7, 8, 12, 20 and 50 μM). (D) Plot of maximum absorbances (indicated by the cyan line) for the Cy-BN-5/38-GC complex *vs.* concentration of quinine (0, 1.5, 2.5, 3.5, 4.5, 5.5, 6.5, 7, 8, 12, 20 and 50 μM) in pH 7.4 HEPES solutions. n = 3.

than that of the colorimetric assay. This work further verifies the generality of the aptamer-based dye-displacement assay and highlights the potential of combining J-aggregate-forming NIR-II cyanine dyes with aptamer-based displacement assays to create sensitive and spectroscopically tuneable sensors (Scheme 1).

DNA aptamer 38-GC can bind to an antimalarial drug quinine with a dissociation constant K_D of 2.4 ± 0.1 μM in its binding buffer.[7c,12] In this study, we tried to find a suitable NIR-II J-aggregating cyanine to form a complex with aptamer 38-GC and achieve optical (both colorimetric and fluorescence) detection as well as fluorescence imaging of quinine. First, we tried our previously obtained J-aggregating dyes to see if they can work with 38-GC to detect quinine by measuring the absorption spectra of our cyanines (compounds **9**, **17** and **23**) upon addition of DNA aptamer 38-GC of varied concentrations in HEPES buffer, as presented in Fig. S1 (SI). It turns out that the addition of 38-GC could hardly interfere with the J-aggregation of the three cyanines in buffer solution, indicating that these three cyanines cannot form a complex with 38-GC and are thus not applicable in dye-displacement assays. We then continued our exploration by fine-tuning the structures of the *meso*-substituent of our cyanines. 5 new cyanines (from Cy-BN-1 to Cy-BN-5, shown in Fig. S2, SI) have been obtained and well-characterized (with their ^{1}H and ^{13}C NMR and HR-MS spectra listed in Fig. S3–S17, SI). We tested their capability of J-aggregation and forming a complex with the 38-GC aptamer. As demonstrated in Fig. S18 (SI) and Fig. 1A, among the five new cyanines, Cy-BN-1 and Cy-BN-5 can self-assemble into J-aggregates in HEPES buffer (containing 5 v/v% or 10 v/v% of DMSO), and only the latter can form a perfect J-aggregate. We tested Cy-BN-5's capability of forming a complex with 38-GC. Fig. 1B shows the absorption spectra of Cy-BN-5 in HEPES solution upon addition of 38-GC of varied concentrations. The presence of 38-GC substantially reduces the absorption band at *ca.* 1040 nm (the J-band of the cyanine), and causes the emergence of an absorption band at around 750 nm (the H-aggregation band). With the concentration ratio of dye to aptamer at 1 : 2, the absorption peak at 1044 nm completely disappears. This result suggests that the aptamer can disrupt the J-aggregates and form a complex with the dye molecules in HEPES buffer. Some forces, such as π–π stacking, hydrophobic and electrostatic interactions, may contribute to the binding between Cy-BN-5 and the 38-GC aptamer.[1e] Next, we prepared a Cy-BN-5/38-GC (1 : 2) complex and tested its spectral response to quinine. As shown in Fig. 1C, the Cy-BN-5/38-GC complex exhibits a characteristic response to quinine in the buffer system. When the concentration of quinine was increased from 0 μM to 200 μM, the absorption peak of the J-aggregate at 1044 nm gradually enhanced, whereas the absorption band of the H-aggregate at 750 nm synchronously attenuated, suggesting that the higher affinity between the aptamer and quinine resulted in the release of quinine molecules into the solution. To rule out the possibility that the pure Cy-BN-5 can detect quinine alone, varied amounts of quinine were added into HEPES solution of Cy-BN-5, and the subsequent absorption measurement (Fig. S19, SI) shows that Cy-BN-5 cannot detect quinine alone. The released Cy-BN-5 molecules rapidly assembled to form J-aggregates. The formed J-aggregates exhibit much higher photostability than ICG (Fig. S20, SI) and its fluorescence quantum yield has been determined as 0.39%. The absorbance of J-aggregates at around 1044 nm in Fig. 1C was plotted against quinine concentration in Fig. 1D, while Fig. S21 (SI) demonstrates a linear fitting curve of the maximum absorbance of J-aggregates with quinine concentration in the linear region. The results show that the maximum absorbances for the dye J-aggregates are significantly linearly correlated with

quinine concentrations in the range of 0 to 7 μM. It was calculated that the absorbance-based limit of detection (LOD) of this dye replacement analysis was 0.35 μM in HEPES buffer solution. This result confirms that the dye/aptamer complex can serve as a dye-replacement assay to detect quinine spectrally in the NIR-II region.

The dissociation constant K_d between the aptamer and Cy-BN-5 complex was determined as 16.9 ± 0.5 μM (Fig. S22, SI), which is much higher than that between the aptamer and quinine (2.4 μM)[7c] under the same conditions, verifying the feasibility of the dye-displacement process in the presence of quinine. We tried to observe the size and morphology of the Cy-BN-5/38-GC complex before and after exposure to quinine. As shown in Fig. S23 (SI), only after quinine treatment, J-aggregate particles form, which can then be observable by DLS and TEM. Moreover, the investigation on the effect of ionic strength on both the J-aggregation and the response behaviour (Fig. S24, SI) shows that the sensor itself, its response to quinine and the J-aggregation can withstand a high ionic strength environment (300 mM of NaCl). To evaluate the selectivity of the Cy-BN-5/aptamer complex for the quinine assay, the absorption spectra of the Cy-BN-5/38-GC complex were determined after mixing with either quinine or a potential interfering substance. As shown in Fig. S25 (SI), the measurement of absorbance at 1044 nm reveals a significant increase in absorbance only in the presence of quinine, while the absorbances for other potential interfering substances shows no significant difference compared to the control, verifying the high selectivity for the quinine assay.

To investigate the capability of the Cy-BN-5/aptamer complex in detecting quinine under simulated physiological conditions, HEPES buffer solutions containing fetal bovine serum (FBS) (2%, w/v) and synthetic urine (2.5%, v/v) were prepared. First, the J-aggregation of Cy-BN-5 in the FBS and urine solutions was tested. As shown in Fig. S26 (SI), Cy-BN-5 could form J-aggregates in both FBS and urine solutions with their absorption spectra slightly or moderately changed compared to those in HEPES buffer, which indicates that Cy-BN-5 exhibits a high tendency of forming J-aggregates in simulated physiological conditions and it is potentially applicable in dye displacement assays in these solutions. The spectrometric assays of quinine by using the Cy-BN-5/38-GC complex in the FBS and urine solutions are presented in Fig. 2. In FBS and urine-containing buffers, the maximum absorbance at around 1000 nm (Fig. 2A, for FBS) and 1050 nm (Fig. 2C, for urine) corresponding to the J-aggregate peaks of Cy-BN-5 gradually increased with rising quinine concentrations. The relationship between maximum absorbances (in FBS and in urine) and quinine concentration are depicted in Fig. 2B and C, while linear ranges for the curves are presented in Fig. S27 and S28 (SI), respectively. And the absorbance-based LOD for this displacement assay in FBS and synthetic urine was calculated to be 0.43 μM and 0.37 μM, respectively. Due to the interference of biological substances in FBS and urine, the LODs for the quinine assay are higher than that in pure HEPES buffer, but they are very much lower than that in the urine of malaria

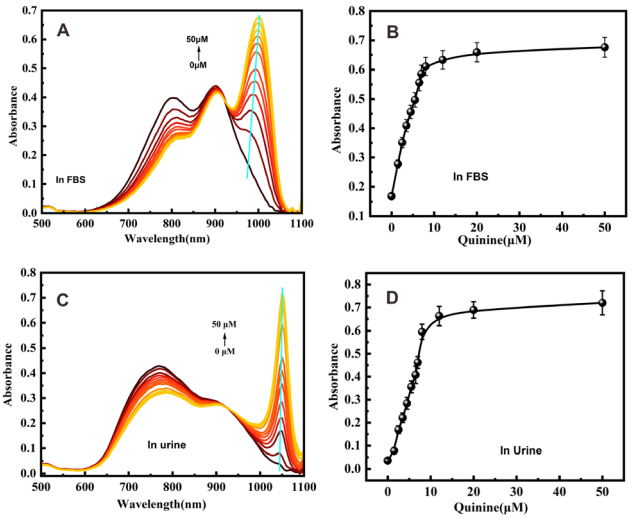

Fig. 2 Absorption spectra of the Cy-BN-5/38-GC complex after addition into quinine solutions with varied concentrations (0, 1.5, 2.5, 3.5, 4.5, 5.5, 6.5, 7, 8, 12, 20 and 50 μM) in HEPES solutions with 2% (w/v) FBS (A) and in HEPES solutions with 2.5% (v/v) synthetic urine (C). Plot of maximum absorbances (indicated by the cyan lines) for Cy-BN-5/38-GC *vs.* concentrations of quinine (0, 1.5, 2.5, 3.5, 4.5, 5.5, 6.5, 7, 8, 12, 20 and 50 μM) in HEPES buffer with 2% (w/v) FBS (B) and in HEPES solution with 2.5% (v/v) synthetic urine (D). n = 3.

patients.[13] This is likely attributable to the exceptional J-aggregate formation capability of Cy-BN-5 in biological fluids.

Considering the higher sensitivity of fluorescence detection, we have further evaluated the fluorescence detection of quinine using the Cy-BN-5/38-GC complex in HEPES buffer containing 2.0% (w/v) FSB and 2.5% (v/v) synthetic urine. As shown in Fig. 3A and B, in the absence of quinine, the Cy-BN-5/38-GC complex displayed almost no fluorescence emission within the NIR-II region, as there was no J-aggregate of Cy-BN-5 formed in

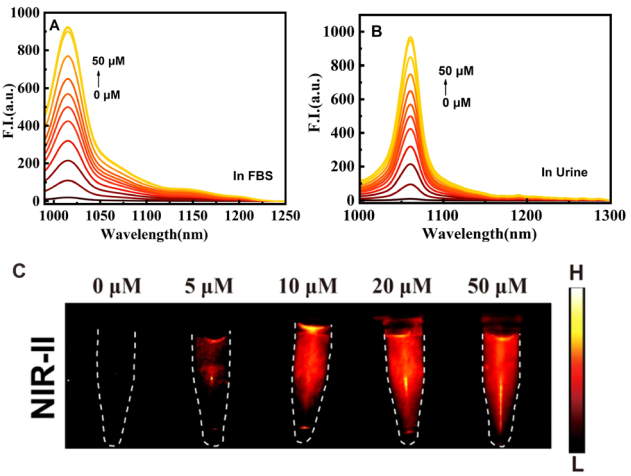

Fig. 3 Fluorescence spectra of the Cy-BN-5/38-GC complex after addition into quinine solutions with varied concentrations in HEPES buffer with 2% (w/v) FBS (A) and in HEPES buffer with 2.5% (v/v) synthetic urine (B). Excitation wavelength: 980 nm; (C) NIR-II fluorescence images of the Cy-BN-5/38-GC complex in the presence of quinine of varied concentrations. Excited with a 980 nm laser.

the FSB or urine-containing buffer solutions. When quinine was added into the solutions, a distinct NIR-II fluorescence peak emerged at 1015 nm (in FSB) or 1062 nm (in synthetic urine), which corresponded to the emission peaks of J-aggregates formed in the two solutions because of the replacement of dye molecules by quinine. The fluorescence intensities of the J-aggregates at around 1015 nm and 1062 nm gradually increased with increasing quinine concentrations. The fluorescence enhancement (FE) factors in FBS and in urine are calculated as 45 and 97, respectively. The correlations between fluorescence intensity at 1015 nm (or 1062 nm) and quinine concentration are plotted in Fig. S29 and S30 (SI), respectively. A linear relationship was observed over the concentration range of 0–8 μM in both FSB and urine-containing buffers. The calculated fluorescence-based LOD for this displacement assay was 0.018 μM (in FSB) and 0.014 μM (in synthetic urine), respectively, reflecting the sensitive fluorescence detection of quinine by using the dye/aptamer complex. Moreover, fluorescence detection in the NIR-II window effectively minimizes interference from endogenous substances such as hemoglobin in biological fluids and significantly reduces tissue autofluorescence.

Given that the J-aggregate emission band of the Cy-BN-5 dye is located at 1062 nm, we further explored its application in NIR-II fluorescence imaging *in vitro*. The Cy-BN-5/38-GC complex was added to HEPES buffer solutions containing varied concentrations of quinine and placed in centrifuge tubes. Imaging was performed with a 980 nm laser for excitation. As shown in Fig. 3C, the fluorescence intensities increase progressively with rising quinine concentrations. This indicates that, upon displacement by quinine, Cy-BN-5 was released from the aptamer complex into solution, where it self-assembled into J-aggregates, generating a detectable fluorescence signal. A comparison between this sensor and some others is presented in Table S1, SI.

In conclusion, we developed a NIR-II aptamer-based dye-displacement assay by integrating a quinine-binding aptamer (38-GC) with a J-aggregating cyanine dye (Cy-BN-5). The displacement of Cy-BN-5 upon quinine recognition triggered the formation of NIR-II-emissive J-aggregates, enabling both colorimetric and fluorescence-based detection. The system demonstrated excellent sensitivity and selectivity, achieving low fluorescence-based LOD, significantly outperforming absorption-based assays. Its robust performance in biological fluids and capability for NIR-II fluorescence imaging highlight the platform's promise for biomedical sensing applications. This study not only validates the feasibility of using J-aggregating dyes in aptamer-based assays, but also paves the way for future development of high-performance biosensors in the NIR-II window.

G. Deng and C. Zhang: conceptualization, data curation, formal analysis, investigation and writing – original draft. J. Chen: investigation, formal analysis and data curation. F. Zeng: conceptualization, formal analysis, supervision, funding acquisition and writing – reviewing & editing. S. Wu: conceptualization, formal analysis, supervision, funding acquisition and writing – reviewing & editing.

This work is financially supported by NSFC (22274057 and 52373209), the Fund of Guangdong Provincial Key Laboratory of Luminescence from Molecular Aggregates (2023B12120 60003).

Conflicts of interest

There are no conflicts to declare.

Data availability

The data supporting this article have been included as part of the SI. Experimental details, synthesis route, NMR spectra and mass spectra, and absorption and emission spectra. See DOI: **https://doi.org/10.1039/d5cc03180j**.

Notes and references

1 (*a*) Y. Lee, J. Buchheim, B. Hellenkamp, D. Lynall, K. Yang, E. F. Young, B. Penkov, S. Sia, M. N. Stojanovic and K. L. Shepard, *Nat. Nanotechnol.*, 2024, **19**, 660; (*b*) K. Yang, N. M. Mitchell, S. Banerjee, Z. Cheng, S. Taylor, A. M. Kostic, I. Wong, S. Sajjath, Y. Zhang, J. Stevens, S. Mohan, D. W. Landry, T. S. Worgall, A. M. Andrews and M. N. Stojanovic, *Science*, 2023, **380**, 942; (*c*) C. Tuerk and L. Gold, *Science*, 1990, **249**, 505; (*d*) A. D. Ellington and J. W. Szostak, *Nature*, 1990, **346**, 818; (*e*) H. Yu, O. Alkhamis, J. Canoura, Y. Liu and Y. Xiao, *Angew. Chem., Int. Ed.*, 2021, **60**, 16800.
2 (*a*) T. Hermann and D. J. Patel, *Science*, 2000, **287**, 820; (*b*) M. Li, F. F. Yin and L. Song, *Chem. Rev.*, 2021, **121**, 10469; (*c*) A. V. Lakhin, V. Z. Tarantul and L. V. Gening, *Acta Naturae*, 2013, **5**, 34.
3 (*a*) R. Stoltenburg, C. Reinemann and B. Strehlitz, *Biomol. Eng.*, 2007, **24**, 381; (*b*) M. Kohlberger and G. Gadermaier, *Biotechnol. Appl. Biochem.*, 2022, **69**, 1771.
4 (*a*) M. N. Stojanovic and D. W. Landry, *J. Am. Chem. Soc.*, 2002, **124**, 9678; (*b*) R. Pei and M. N. Stojanovic, *Anal. Bioanal. Chem.*, 2008, **390**, 1093; (*c*) O. Alkhamis, J. Canoura, H. Yu, Y. Liu and Y. Xiao, *Trends Anal. Chem.*, 2019, **121**, 115699; (*d*) Y. Tan, X. Zhang, Y. Xie, R. Zhao, C. Tan and Y. Jiang, *Analyst*, 2012, **137**, 2309; (*e*) C. Zhou, Y. Jiang, S. Hou, B. Ma, X. Fang and M. Li, *Anal. Bioanal. Chem.*, 2006, **384**, 1175; (*f*) Y. Jiang, X. Fang and C. Bai, *Anal. Chem.*, 2004, **76**, 5230.
5 (*a*) A. D. Keefe, S. Pai and A. Ellington, *Nat. Rev. Drug Discovery*, 2010, **9**(7), 537; (*b*) M. Safarkhani, S. Ahmadi, H. Ipakchi, M. R. Saeb, P. Makvandi, M. E. Warkiani, N. Rabiee and Y. S. Huh, *Adv. Sci.*, 2024, **11**, 2401617; (*c*) S. Walia, A. R. Chandrasekaran, B. Chakraborty and D. Bhatia, *ACS Appl. Bio Mater.*, 2021, **4**, 5392.
6 M. N. Stojanovic and D. M. Kolpashchikov, *J. Am. Chem. Soc.*, 2004, **126**, 9266.
7 (*a*) Z. Li, S. Zhang, T. Yu, Z. Dai and Q. Wei, *Anal. Chem.*, 2019, **91**, 10448; (*b*) O. Alkhamis, J. Canoura, K. V. Bukhryakov, A. Tarifa, A. P. DeCaprio and Y. Xiao, *Angew. Chem., Int. Ed.*, 2022, **61**, e202112305; (*c*) X. Jin, Y. Liu, O. Alkhamis, J. Canoura, A. Bacon, R. Xu, F. Fu and Y. Xiao, *Anal. Chem.*, 2022, **94**(28), 10082–10090; (*d*) J. Canoura, O. Alkhamis, M. Venzke, P. T. Ly and Y. Xiao, *JACS Au*, 2024, **4**, 1059.
8 (*a*) Y. Meng, K. High, J. Antonello, M. W. Washabaugh and Q. Zhao, *Anal. Biochem.*, 2005, **345**, 227; (*b*) X. Hou, Q. Yu, F. Zeng, J. Ye and S. Wu, *J. Mater. Chem. B*, 2015, **3**, 1042.
9 J. L. Bricks, Y. L. Slominskii, I. D. Panas and A. P. Demchenko, *Methods Appl. Fluoresc.*, 2017, **6**, 012001.
10 C. Zhang, Y. Wu, F. Zeng, Y. Wen, J. Chen, G. Deng, L. Zhang, S. Zhao, S. Wu and Y. Zhao, *Angew. Chem., Int. Ed.*, 2024, **63**, e202406694.
11 (*a*) M. Datta, Y. A. Kaiyum, P. E. Johnson and J. Liu, *Chem. – Eur. J.*, 2024, **30**, e202403435; (*b*) J. A. Adegbola, J. O. Soyinka and B. A. Adeagbo, *Asian J. Pharm. Res. Health Care*, 2016, **8**, 11.
12 O. Reinstein, M. Yoo, C. Han, T. Palmo, S. A. Beckham, M. C. J. Wilce and P. E. Johnson, *Biochemistry*, 2013, **52**, 8652.
13 V. F. Samanidou, E. N. Evaggelopoulou and I. N. Papadoyannis, *J. Pharm. Biomed. Anal.*, 2005, **38**, 21.

